

# Gas-phase tautomers of protonated 1-methylcytosine. Preparation, energetics, and dissociation mechanisms

Chunxiang Yao,<sup>1</sup> Maria L. Cuadrado-Peinado,<sup>1</sup> Miroslav Poláček<sup>2</sup> and František Tureček<sup>1\*</sup>

<sup>1</sup> Department of Chemistry, Bagley Hall, Box 3517090, University of Washington, Seattle, WA 98195-1700, USA

<sup>2</sup> J. Heyrovský Institute of Physical Chemistry, Academy of Sciences of the Czech Republic, Dolejškova 3, 18223 Prague 8, Czech Republic

Received 31 May 2005; Accepted 29 July 2005

Tautomers of 1-methylcytosine that are protonated at N-3 (1<sup>+</sup>) and C-5 (2<sup>+</sup>) have been specifically synthesized in the gas phase and characterized by tandem mass spectrometry and quantum chemical calculations. Ion 1<sup>+</sup> is the most stable tautomer in aqueous and methanol solution and is likely to be formed by electrospray ionization of 1-methylcytosine and transferred in the gas phase. Gas-phase protonation of 1-methylcytosine produces a mixture of 1<sup>+</sup> and the O-2-protonated tautomer (3<sup>+</sup>), which are nearly isoenergetic. Dissociative ionization of 6-ethyl-5,6-dihydro-1-methylcytosine selectively forms isomer 2<sup>+</sup>. Upon collisional activation, ions 1<sup>+</sup> and 3<sup>+</sup> dissociate by loss of ammonia and [C,H,N,O], whose mechanisms have been established by deuterium labeling and *ab initio* calculations. The main dissociations of 2<sup>+</sup> following collisional activation are losses of CH<sub>2</sub>=C=NH and HN=C=O. The mechanisms of these dissociations have been elucidated by deuterium labeling and theoretical calculations. Copyright © 2005 John Wiley & Sons, Ltd.

**KEYWORDS:** nucleobases; cytosine; tandem mass spectrometry; *ab initio* calculations; neutral and ion tautomers

## INTRODUCTION

Nucleobases, nucleosides, and nucleotides have been actively studied by mass spectrometry with the goal of elucidating ion dissociations that could be used for DNA and RNA characterization.<sup>1</sup> McCloskey and coworkers used stable isotope labeling and collision-induced dissociation in several studies that targeted dissociations of protonated uracil,<sup>2</sup> adenine,<sup>3</sup> and guanine.<sup>4</sup> These studies revealed some unexpected features of seemingly simple ion dissociations, as exemplified by the elimination of NH<sub>3</sub> from protonated adenine that almost equally involves nitrogen atoms originating from the NH<sub>2</sub> group and the ring N-1 position.<sup>3</sup> Owing to the advanced stage of quantum chemistry calculations, it has now become possible and practical to elucidate the potential energy surfaces for nucleobase ion dissociations in great detail and thus disclose some unexpected features of fragmentation mechanisms.<sup>5</sup> A complicating factor in the study of nucleobase ions is the presence of tautomers of both neutral nucleobase molecules in the gas phase and also the ions derived therefrom. A case in point is cytosine that exists as three tautomers that interconvert rapidly in the gas phase.<sup>6–11</sup> Gas-phase protonation of the neutral tautomer

mixture is predicted to form an even more complex mixture of ion tautomers,<sup>12</sup> which would impair attempts at mechanistic studies of dissociation mechanisms. Following our recent studies of adenine cation-radicals<sup>13</sup> and cations,<sup>5</sup> we now address the dissociations of protonated cytosine. To simplify this task, we have chosen to study tautomeric cations derived from 1-methylcytosine (*I*) in which the *N*-methyl group prevents keto–enol tautomerization in the neutral molecule which is forced to adopt the canonical 1,2-dihydro-4-aminopyrimidine-2(1*H*)-one ring structure. A small amount of imino–oxo tautomers (*VIIa* and *VIIb*, Fig. 1) has been reported to accompany *I* when deposited from the gas phase in a frozen argon matrix.<sup>14</sup> We use specific ion synthesis to generate two tautomeric cytosine cations, 1-methyl-2-oxo-1,2,3,4-tetrahydro-4-aminopyrimidine-4-yl cation (1<sup>+</sup>) and 1-methyl-4-amino-1,2,5,6-tetrahydropyrimidine-2(1*H*)-on-6-yl cation (2<sup>+</sup>), and implement stable isotope labeling and high-level quantum chemistry calculations to study the mechanisms of their dissociations upon collisional activation. Another motivation for this ion-chemistry study is to use these well-characterized cations as precursors for the specific formation of cytosine radicals by femtosecond electron transfer in the gas phase.<sup>15–17</sup>

## EXPERIMENTAL

### Materials and synthetic procedures

1-Methylcytosine (*I*) was synthesized from cytosine with 65% yield according to literature<sup>18</sup> (Scheme 1).

The product was purified by recrystallization from methanol–petroleum ether and had m.p. 290 °C (lit.<sup>18</sup> 301–302 °C). <sup>1</sup>H NMR (DMSO-*d*<sub>6</sub>, 25 °C): 3.19 (s, 3H, N-CH<sub>3</sub>),

\*Correspondence to: František Tureček, Department of Chemistry, Bagley Hall, Box 3517090, University of Washington, Seattle, WA 98195-1700, USA. E-mail: turecek@chem.washington.edu  
Contract/grant sponsor: National Science Foundation;  
Contract/grant numbers: CHE-0349595; CHE-0342956.  
Contract/grant sponsor: Grant Agency of the Czech Republic;  
Contract/grant number: 203/02/0737.  
Contract/grant sponsor: Grant Agency of the Academy of Sciences of the Czech Republic; Contract/grant number: IAA400400502.

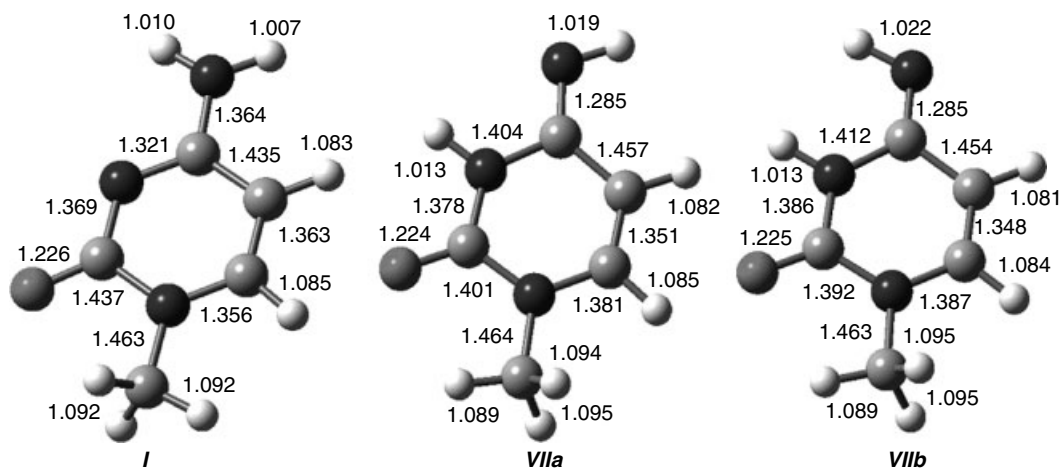
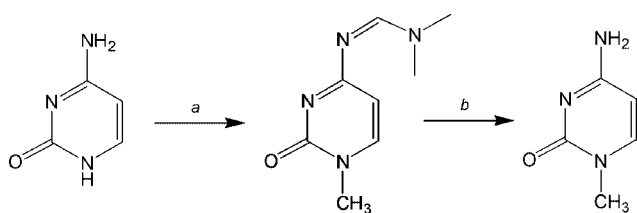


**Figure 1.** B3LYP/6-31+G(d,p) optimized structures of 1-methylcytosine tautomers. Bond lengths in angstroms.



**Scheme 1.** *a*:  $(\text{CH}_3)_2\text{N-CH}(\text{OCH}_3)_2/\text{CF}_3\text{COOH}$ ; *b*:  $\text{NH}_4\text{OH}/\text{H}_2\text{O}$ .

5.61 (d, 1H,  $J = 7.2$  Hz), 6.91 (broad s, 2H,  $\text{NH}_2$ ), 7.55 (d, 1H,  $J = 7.2$  Hz). Mass spectrum ( $m/z$ , % relative intensity): 125(100), 124(6), 111(3), 110(4), 96(5), 83(10), 81(7), 42(11).

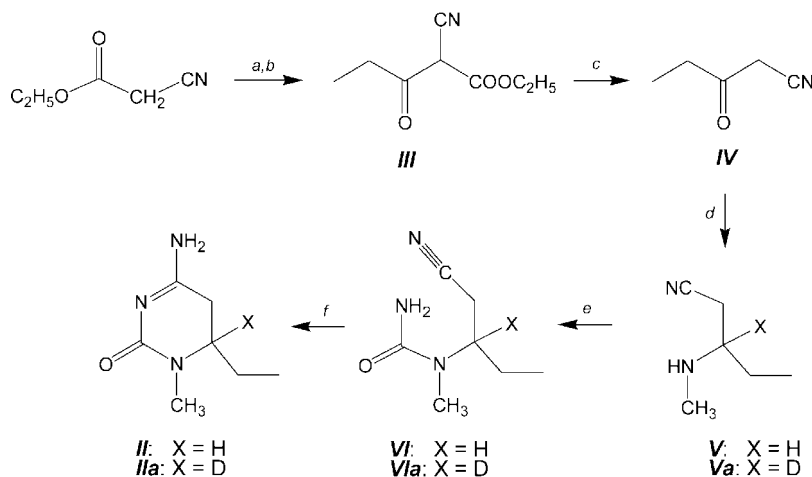
1-Methyl-6-ethyl-5,6-dihydrocytosine (**II**) was synthesized in five steps, as shown in Scheme 2.

Condensation of ethylcyanoacetate with propionyl chloride<sup>19</sup> (both Sigma-Aldrich) gave ethyl 2-cyano-3-oxopentanoate (**III**) which was hydrolyzed and decarboxylated in moist DMSO<sup>20</sup> to give the polar and not very stable 3-oxopentenenitrile **IV**.<sup>19</sup> The latter was purified by careful vacuum distillation and immediately reductively aminated<sup>21,22</sup> with methylamine and sodium cyanoborohydride (Sigma-Aldrich) to provide 3-(methylamino)pentanenitrile (**V**). Reductive amination of

**IV** with methylamine and sodium cyanoborodeuteride (Sigma-Aldrich) gave the deuterated derivative, [3-<sup>2</sup>H]-3-(methylamino)pentanenitrile (**Va**). Nitrile **V** was treated with nitrourea<sup>23</sup> to give the substituted urea **VI**, which was cyclized<sup>24</sup> to **II** upon treatment with sodium amide in dry dioxan. An analogous treatment of **Va** yielded the 6-deutero derivative **IIa**. The synthetic intermediates were characterized by infrared spectroscopy, and mass spectrometry or gas chromatography-mass spectrometry (GC-MS).

### 3-Oxopentenenitrile (**IV**)

A mixture of ethyl cyanoacetate (17.0 g, 0.150 mol), anhydrous magnesium chloride (14.5 g, 0.152 mol), and redistilled triethylamine (30.5 g, 0.301 mol, Fisher) in dry acetonitrile (150 ml, Fisher) was stirred at 0 °C for 15 min. Then propionyl chloride (13.85 g, 0.150 mol) was added dropwise over 15 min. The reaction mixture was allowed to warm up to room temperature and stirred overnight. HCl (30%, 100 ml) was added, the mixture was stirred until the precipitate dissolved, and the product was extracted with ether (3 × 100 ml). The ether phase was washed with water, dried over anhydrous  $\text{Na}_2\text{SO}_4$ , the solvent was evaporated, and the residue was distilled *in vacuo* (0.2 torr) to give 17.7 g (70%) of



**Scheme 2.** *a*:  $\text{MgCl}_2/\text{Et}_3\text{N}$ ; *b*:  $\text{MeCN}, \text{C}_2\text{H}_5\text{COCl}$ ; *c*:  $\text{DMSO}/\text{H}_2\text{O}, 120^\circ\text{C}$ ; *d*:  $\text{X} = \text{H}: \text{CH}_3\text{NH}_2/\text{NaBH}_3\text{CN}/\text{CH}_3\text{OH}$ ; *d*:  $\text{X} = \text{D}; \text{CH}_3\text{NH}_2/\text{NaBD}_3\text{CN}/\text{CH}_3\text{OH}$ ; *e*:  $\text{H}_2\text{NCONHNO}_2/\text{MeOH}/\text{H}_2\text{O}$ ; *f*:  $\text{NaNH}_2/\text{dioxan}$ .

ethyl 2-cyano-3-oxopentanoate (**III**). GC-MS showed essentially one peak, mass spectrum ( $m/z$ , % relative intensity): 169 (47), 141(39), 123(44), 112(92), 95(52), 68(69), 57(100).

Compound **III** (17.6 g) was dissolved in 50 ml of 90% DMSO and 10% water and the mixture was heated under argon at 120 °C until the evolution of CO<sub>2</sub> ceased. The mixture was cooled to 0 °C, saturated NaCl solution (250 ml) was added, and the product was extracted with 3 × 50 ml of CH<sub>2</sub>Cl<sub>2</sub>. The dichloromethane extract was dried over anhydrous Na<sub>2</sub>SO<sub>4</sub>, the solvent was evaporated, and the residue was distilled *in vacuo* (0.2 torr) to give 8.6 g (85%) of 3-oxopentanenitrile (**IV**). IR (neat, cm<sup>-1</sup>) $\nu_{\max}$ : 1630 (C=O), 2247 (CN). Mass spectrum ( $m/z$ , % relative intensity): 68 (16), 57(48), 42(9), 41(15), 40(22), 39(9), 29(100), 27(42).

### 3-(Methylamino)pentanenitrile (**V**)

A solution of **IV** (8.5 g, 87.5 mmol) in 30 ml methanol was mixed with 50 ml of 2M methylamine solution in methanol and the mixture was stirred at room temperature for 15 min. Then a solution of sodium cyanoborohydride (2.2 g, 35 mmol) in 25 ml of methanol was added dropwise over 30 min under stirring. After another 30 min, the reaction mixture was added with solid KOH (15 g), and the volume was reduced to 50 ml on a rotary evaporator. Water (10 ml) and saturated brine (25 ml) were added, the organic layer was separated, and the aqueous layer was extracted with 2 × 50 ml of ether. The combined organic layers were extracted with 3 × 20 ml of 20% HCl. The HCl extract was cooled to 0 °C, made basic by adding solid NaOH, and extracted with 3 × 20 ml of ether. The ether extract was washed with saturated brine, dried over K<sub>2</sub>CO<sub>3</sub>, ether was distilled off *in vacuo*, and the crude product was purified by vacuum distillation (150 °C/0.2 torr) to give 0.40 g (4%) of **V**. IR (neat, cm<sup>-1</sup>): 2261 (CN), 3447 (NH); GC-MS gave essentially one peak (>95%). Mass spectrum ( $m/z$ , % relative intensity): 83(78), 73(15), 72(100), 57(28), 56(15), 44(12), 42(74), 41(15), 30(31), 28(32).

### [3-<sup>2</sup>H<sub>1</sub>]-3-(Methylamino)pentanenitrile (**Va**)

**Va** was prepared analogously from **IV** using sodium cyanoborodeuteride. Mass spectrum ( $m/z$ , % relative intensity): 84(75), 83(16), 73(100), 72(31), 58(25), 57(24), 43(72), 42(65), 30(32), 29 (18), 28(17).

### *N*-(1-Cyano-2-butyl)-*N*-methylurea (**VI**)

Nitrile **V** (0.39 g, 3.5 mmol) was stirred with nitrourea (0.56 g, 5.3 mmol) in 10 ml of 4:1 water/methanol at 50 °C for 1 h. The solvent was removed on a rotary evaporator to give a solid residue (0.49 g, 90%). Mass spectrum ( $m/z$ , % relative intensity): 126(3), 115(46), 83(54), 72(100), 57(12), 56(13), 44(23), 42(46), 30(12). IR(cm<sup>-1</sup>): 1653 (C=O), 2250 (CN), 3448 (NH).

### *N*-([2-<sup>2</sup>H<sub>1</sub>]-1-Cyano-2-butyl)-*N*-methylurea (**VIa**)

**VIa** was prepared analogously from **Va**. Compound **VIa** gave essentially a single peak on GC-MS (>95%): Mass spectrum ( $m/z$ , % relative intensity): 127(3), 116(46), 115(10), 84(47), 83(12), 73(100), 72(22), 58(12), 57(14), 56(11), 44(29), 43(36), 42(28), 31(5), 30(15).

### 1-Methyl-6-ethyl-5,6-dihydrocytosine (**II**)

Compound **VI** (0.55 g, 3.5 mmol) was dissolved in a minimum volume of hot dioxane (5 ml), one crystal of sodium amide (20 mg) was added to the solution, and the mixture was maintained at 70 °C overnight under stirring. Product **II** that crystallized upon cooling was collected and the supernatant was placed at 4 °C to yield a second crop of crystalline **II**. Total yield: 0.41 g (73%). Mass spectrum ( $m/z$ , % relative intensity): 155(11), 126(100), 85(15), 83(43), 42(28). <sup>1</sup>H-NMR(DMSO-*d*<sub>6</sub>, 25 °C): 0.82 (t, 3H, CH<sub>3</sub>CH<sub>2</sub>-), 1.28, 1.53 (m, 2H, CH<sub>3</sub>-CH<sub>2</sub>-), 2.34 (d, 1H, *J* = 15 Hz, H<sub>eq</sub>-5), 2.52 (dd, 1H, *J* = 15 and 7.5 Hz, H<sub>ax</sub>-5), 2.82 (br s, 3H, N-CH<sub>3</sub>), 3.23 (m, 1H, H-6), 7.21(br s, 1H), 7.43(br s, 1H).

### 1-Methyl-6-ethyl-[6-<sup>2</sup>H<sub>1</sub>]-5,6-dihydrocytosine (**IIa**)

**IIa** was prepared analogously from **VIa**. Mass spectrum ( $m/z$ , % relative intensity): 156.1121 (C<sub>7</sub>H<sub>12</sub>N<sub>3</sub>OD requires 156.1118, M, 15%), 155 (3), 127(100), 126(24), 86(12), 84(29), 43(19), 42(11). <sup>1</sup>H-NMR(DMSO-*d*<sub>6</sub>, 25 °C): 0.82 (t, 3H, CH<sub>3</sub>CH<sub>2</sub>-), 1.28, 1.53 (m, 2H, CH<sub>3</sub>-CH<sub>2</sub>-), 2.33 (d, 1H, *J* = 15 Hz, H<sub>eq</sub>-5), 2.53 (d, 1H, *J* = 15 Hz, H<sub>ax</sub>-5), 2.82 (br s, 3H, N-CH<sub>3</sub>).

### 1-Methyl-6-ethyl-[5,*N*-<sup>2</sup>H<sub>2</sub>]-5,6-dihydrocytosine (**IIb**)

Compound **II** (260 mg) was dissolved in a 1:1 mixture of D<sub>2</sub>O and CD<sub>3</sub>OD (10 ml) that contained K<sub>2</sub>CO<sub>3</sub> to adjust to pH 9. The mixture was kept in the dark at room temperature for 3 days. Then it was acidified with CD<sub>3</sub>COOD, the solvents were reduced on a rotary evaporator, the product was extracted with acetonitrile, and the solvent was evaporated. An aliquot of the deuterated intermediate (170 mg) was dissolved in 3 ml of a 4:1 methanol-water mixture and the solution was stirred at room temperature for 1 h. The solvents were removed and the solid product was characterized by <sup>1</sup>H-NMR (DMSO-*d*<sub>6</sub>, 25 °C): 0.84 (t, 3H, CH<sub>3</sub>CH<sub>2</sub>-), 1.42, 1.58 (m, 2H, CH<sub>3</sub>-CH<sub>2</sub>-), 2.52 (d, 1H), 2.89 (br s, 3H, N-CH<sub>3</sub>), 3.38 (dd, 1H, *J* = 4.8 and 8.1 Hz, H-6). Mass spectrum ( $m/z$ , % relative intensity): 158(7), 157 (17), 156(23), 155(14), 129(22), 128(61), 127(88), 126(57), 86(14), 85(27), 84(41), 83(31), 42(100). This showed that the product was a mixture of mainly D<sub>1</sub> and D<sub>2</sub> species that, rather unexpectedly, had an axial proton and an equatorial deuteron at C-5.

## Methods

<sup>1</sup>H-NMR spectra were measured on a Bruker Avance 300 spectrometer at 300.13 MHz in DMSO-*d*<sub>6</sub> at 25 °C. GC-MS was performed on an HP 5971A instrument equipped with a silicone elastomer DB5 GC capillary column. Electron and chemical ionization mass spectra were measured on a JEOL HX-110 double-focusing mass spectrometer of an EB geometry (electrostatic sector E precedes magnet B). Samples were introduced from a heated solid probe at 120–150 °C. The ion source temperature was 200 °C. EI ionization conditions were as follows: emission current, 100 μA; electron energy, 70 eV; acceleration voltage, 10 kV. Chemical ionization (CI) mass spectra were obtained with NH<sub>3</sub>/NH<sub>4</sub><sup>+</sup> or ND<sub>3</sub>/ND<sub>4</sub><sup>+</sup> as the ionization reagents. Collisionally activated dissociation (CAD) spectra were obtained with air as a collision gas, which was admitted

in the first field region at pressures allowing 70 and 50% transmittance of the ion beam. The spectra were recorded by scanning B and E while keeping their ratio constant (B/E linked scan). The mass resolution was adjusted as needed, e.g. >10 000 for accurate mass measurements in both regular and B/E mass spectra and >500 in low-resolution mass spectra. Electrospray ionization-CAD spectra were measured on a Micromass Quattro II tandem quadrupole mass spectrometer (Q1q2Q3). Samples were sprayed from  $10^{-4}$  M solutions in methanol or CD<sub>3</sub>OD. CAD spectra (Ar, multiple collision conditions) of mass-selected ions were obtained at 4, 8, 12, 15, and 23 eV laboratory collision energies ( $E_{\text{LAB}}$ ) by setting an appropriate voltage bias between the collision radiofrequency-only quadrupole (q2) and the mass-selecting quadrupole mass filter (Q1). Spectra were obtained by scanning Q3 at unit mass resolution. For  $m/z$  126 precursor ions, these  $E_{\text{LAB}}$  correspond to 1, 2, 3, 3.6, and 5.6 eV center-of-mass collision energies,  $E_{\text{COM}} = E_{\text{LAB}} \times 40 / (40 + 126)$ .

Another set of spectra were obtained on a ZAB2-SEQ tandem-hybrid mass spectrometer of a reverse double-focusing geometry (B precedes E), which is equipped with a collision quadrupole and a quadrupole mass analyzer for low-energy CAD measurements of ions passing through BE. Precursor ions were produced by electron ionization at 70 eV or by chemical ionization using (CH<sub>3</sub>)<sub>3</sub>N/(CH<sub>3</sub>)<sub>3</sub>NH<sup>+</sup>, NH<sub>3</sub>/NH<sub>4</sub><sup>+</sup>, or ND<sub>3</sub>/ND<sub>4</sub><sup>+</sup> as reagents. Ions were accelerated to a kinetic energy of 8 keV and activated by collisions with He that was admitted to the first field-free region at pressures to achieve 50% transmittance of the precursor ion beam. CAD spectra were obtained by a linked scan of B and E. Low-energy CAD spectra were obtained by selecting ions by BE, decelerating them to the desired kinetic energy ( $E_{\text{LAB}} = 10, 20, \text{ and } 30 \text{ eV}$ ), and allowing them to collide with air in a radio frequency-only quadrupole. For  $m/z$  126 precursor ions, these  $E_{\text{LAB}}$  corresponded to 1.8, 3.6, and 5.5 eV center-of-mass collision energies,  $E_{\text{COM}} = E_{\text{LAB}} \times 28 / (28 + 126)$ . Product ion mass spectra were obtained by scanning the final quadrupole mass filter at unit mass resolution.

## Calculations

Standard *ab initio* and density functional theory calculations were performed using the Gaussian 03 suite of programs.<sup>25</sup> Geometries were optimized with Becke's hybrid functional (B3LYP)<sup>26–28</sup> using the 6–31+G(d,p) basis set. The optimized structures for the most relevant species are shown in Figs 1 and 6 (complete geometries in the Cartesian coordinate format can be obtained from the corresponding author upon request). The same level of theory was used for frequency analysis to characterize local energy minima (all real frequencies) and transition states as first-order saddle points (one imaginary frequency). Improved energies were obtained by single-point calculations using B3LYP and Moller–Plesset theory<sup>29</sup> truncated at second order (MP2, frozen core) and the larger triple- $\zeta$  split valence 6–311+G(2d,p) and 6–311++G(3df,2p) basis sets furnished with multiple shells of polarization functions at C, NO, and H and shells of s and p diffuse functions at C, N, O, and H. Calculations with the two basis sets gave

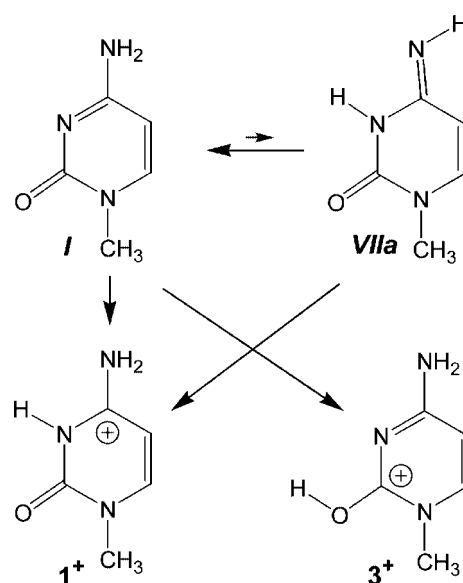
very similar relative energies. The B3LYP and MP2 single-point energies were averaged according to the previously reported B3-MP2 scheme<sup>30</sup> that has been shown to achieve improved accuracy at the level of highly correlated composite *ab initio* methods by canceling small errors inherent to the B3LYP and MP2 approximations.<sup>31–38</sup> The B3-MP2 energies were used to calculate relative energies that were corrected for zero-point vibrational contributions. The reported relative energies thus correspond to 0 K unless stated otherwise. Enthalpy corrections and entropies were calculated from B3LYP/6–31+G(d,p) harmonic frequencies and moments of inertia within the rigid rotor–harmonic oscillator approximation.

Solvation free energies were calculated using the refined Polarizable Continuum Model (PCM) of Tomasi *et al.*<sup>39,40</sup> included in Gaussian 03. As noted in the program, this PCM model is different from that included in Gaussian 98,<sup>41</sup> and the free energies from these two models should not be mixed.

## RESULTS AND DISCUSSION

### 1-Methylcytosine tautomers and protonation sites

We use gas-phase and solution protonation of 1-methylcytosine to generate the ions of interest and study their gas-phase chemistry. Thus, both the structure of neutral 1-methylcytosine (*I*) and the protonation sites in *I* are of importance and have to be addressed first. According to the literature,<sup>14</sup> when deposited from the gas phase at 463 K, 1-methylcytosine consists of a mixture of *I* and the (*E*) and (*Z*) imine isomers *VIIa* and *VIIb*, respectively (Fig. 1). We calculated the relative free energies of these three isomers at 298 K and 473 K, as shown in Table 1. The data indicate that there are 7 and 1% of *VIIa* and *VIIb*, respectively, at equilibrium with 92% of *I* at 473 K, but less than 2% total of *VIIa* and *VIIb* at 298 K. This indicates that evaporating *I* at the typical ion source temperatures (453–473 K) may result in co-sampling of up to 8% of imine tautomers *VIIa* and *VIIb*. In contrast, the canonical tautomer *I* shows a substantially greater



Scheme 3

solvation free energy in aqueous and methanol solutions than do *VIIa* and *VIIIb*, which results in equilibrium that greatly favors *I* (~99.9%, Table 1). This finding is important for ionization of 1-methylcytosine by electrospray, which takes place in solution where tautomer *I* is predicted to dominate.

The protonation sites in *I* and *VIIa* are assessed from the calculated topical gas-phase basicities and solvation energies (Table 2). These show that the major tautomer *I* has practically identical gas-phase basicities for the O-2 and N-3 positions (930 and 931 kJ mol<sup>-1</sup>, respectively). Thus, positions N-3 and O-2 in *I* are expected to be competitively

attacked by a gas-phase acid, giving rise to isomeric ions 1<sup>+</sup> and 3<sup>+</sup> (Scheme 3).

Positions C-5, N-7, N-1, and C-6 are substantially less basic than N-3/O-2 and cannot be protonated competitively with mild gas-phase acids, such as (CH<sub>3</sub>)<sub>3</sub>NH<sup>+</sup> or NH<sub>4</sub><sup>+</sup>. This means that the corresponding ion isomers 2<sup>+</sup>, 4<sup>+</sup>, 5<sup>+</sup>, and 6<sup>+</sup> are not accessible by selective gas-phase protonation of *I*. The topical gas-phase basicities in *VIIa* show great preference for protonation at N-7, giving rise to ion 1<sup>+</sup> while the isomeric ion 7<sup>+</sup> is substantially less stable than 1<sup>+</sup>.

In contrast to the gas phase, protonation of tautomer *I* in aqueous and methanol solutions is predicted to occur at N-3

**Table 1.** Relative enthalpies and free energies of *N*-methylcytosine tautomers

Tautomer	$\Delta H_{g,0}^{a,b}$	$\Delta G_{g,298}^c$	$\Delta G_{g,473}^d$	$\Delta G_{solv,298}^e$	$\Delta G_{sol,298}^f$
<i>I</i>	0	0 (98.3%)	0 (92%)	-83 <sup>g</sup> -79 <sup>h</sup>	0 (99.9%) 0 (99.9%)
<i>VIIa</i>	12.3	10.2 (1.6%)	10.1(7%)	-68 <sup>g</sup> -65 <sup>h</sup>	35 (0.00%) 24 (0.01%)
<i>VIIIb</i>	19.8	17.8 (0.1%)	17.9 (1%)	-71 <sup>g</sup> -68 <sup>h</sup>	18 (0.08%) 18 (0.08%)

<sup>a</sup> All energies in units of kJ mol<sup>-1</sup>.

<sup>b</sup> Gas-phase relative enthalpies at 0 K from B3-MP2/6-311++G(3df,2p) single-point energies and B3LYP/6-31+G(d,p) zero-point energy corrections.

<sup>c</sup> Gas-phase relative free energies at 298 K. The values in parentheses are the equilibrium fractions.

<sup>d</sup> Gas-phase relative free energies at 473 K.

<sup>e</sup> Solvation energies calculated with B3LYP/6-31+G(d,p) and the Polarizable Continuum Model.

<sup>f</sup> Relative free energies in solution at 298 K.

<sup>g</sup> Solvation in water.

<sup>h</sup> Solvation in methanol.

**Table 2.** Gas-phase and solution basicities of *I* and *VIIa*

Tautomer/ Position	Ion	PA <sup>a</sup>	GB <sup>b</sup>	$\Delta G_{g,rel}^c$	$\Delta G_{solv}^d$	$\Delta G_{sol,rel}^e$
<i>I</i>						
N-3	1 <sup>+</sup>	964	931	0	-281 <sup>f</sup> (-274) <sup>g</sup>	0
C-5	2 <sup>+</sup>	852	823	108	-277 <sup>f</sup> (-270) <sup>g</sup>	112 <sup>f</sup> (112) <sup>g</sup>
O-2	3 <sup>+</sup>	964	930	0.7	-250 <sup>f</sup> (-243) <sup>g</sup>	32 <sup>f</sup> (31) <sup>g</sup>
N-7	4 <sup>+</sup>	836	805	126	-315 <sup>f</sup> (-306) <sup>g</sup>	92 <sup>f</sup> (93) <sup>g</sup>
N-1	5 <sup>+</sup>	803	772	158	-	-
C-6	6 <sup>+</sup>	612	584	282	-	-
<i>VIIa</i>						
O-2	7 <sup>+</sup>	854	822	120	-279 <sup>f</sup> (-272) <sup>g</sup>	122 <sup>f</sup> (122) <sup>g</sup>
N-7	1 <sup>+</sup>	975	942	0	-	-

<sup>a</sup> Topical gas-phase proton affinities at 298 K from B3-MP2/6-311++G(3df,2p) single-point energies and B3LYP/6-31+G(d,p) zero-point energy corrections and enthalpies. All energies are in units of kJ mol<sup>-1</sup>.

<sup>b</sup> Topical gas-phase basicities at 298 K.

<sup>c</sup> Relative ion gas-phase free energies at 298 K.

<sup>d</sup> Solvation free energies.

<sup>e</sup> Relative ion free energies in solution.

<sup>f</sup> Solvation in water.

<sup>g</sup> Solvation in methanol.

with a high selectivity. This is mainly due to the substantially greater solvation free energy of the oxo-tautomer  $1^+$  compared to the 'enol'-tautomer  $3^+$ . The calculated free energy differences,  $\Delta G_{\text{aq}}(1^+ \rightarrow 3^+) = 31.7$  and  $31.2 \text{ kJ mol}^{-1}$  in water and methanol, respectively, indicate  $>99.9\%$  of  $1^+$  at 298 K equilibrium in solution. These results are perfectly consistent with the previous  $^1\text{H-NMR}$  study that showed that *I* was protonated at N-3 in a hydrochloride salt in dimethylsulfoxide solution.<sup>42</sup> The experimental and computational data strongly suggest that solution ionization of 1-methylcytosine should selectively produce ion  $1^+$  as the predominating species by far. Hence, one can expect that electrospray ionization of 1-methylcytosine that occurs in acidic solvent droplets<sup>43</sup> produces mainly isomer  $1^+$ .

Because of its lower stability, ion  $2^+$  cannot be produced competitively with the more stable  $1^+$ . The route to  $2^+$  utilizes  $\alpha$ -cleavage dissociation<sup>44</sup> by loss of the side-chain ethyl group from precursor *II* (Scheme 4). Ion  $2^+$  (measured mass 126.0662,  $\text{C}_5\text{H}_8\text{N}_3\text{O}$  requires 126.0667) represents the base peak of the electron-ionization mass spectrum of *II* (see 'Experimental' section), which provides an abundant source of the desired ion. EI-dissociations of deuterium-labeled isotopomers *IIa* and *IIb* were used to generate ions  $2\text{a}^+$  and  $2\text{b}^+$ , respectively (Scheme 4). The structural integrity of ion  $2^+$  was confirmed by collisionally activated dissociation mass spectra, which are discussed next.

### Dissociations of $1^+$ and $2^+$

CAD mass spectra at  $E_{\text{COM}} = 5.5\text{--}5.6 \text{ eV}$  of  $m/z$  126 ions produced by gas-phase protonation with  $\text{NH}_4^+$ ,  $(\text{CH}_3)_3\text{NH}^+$ , and by electrospray ionization of *I* were very similar, as

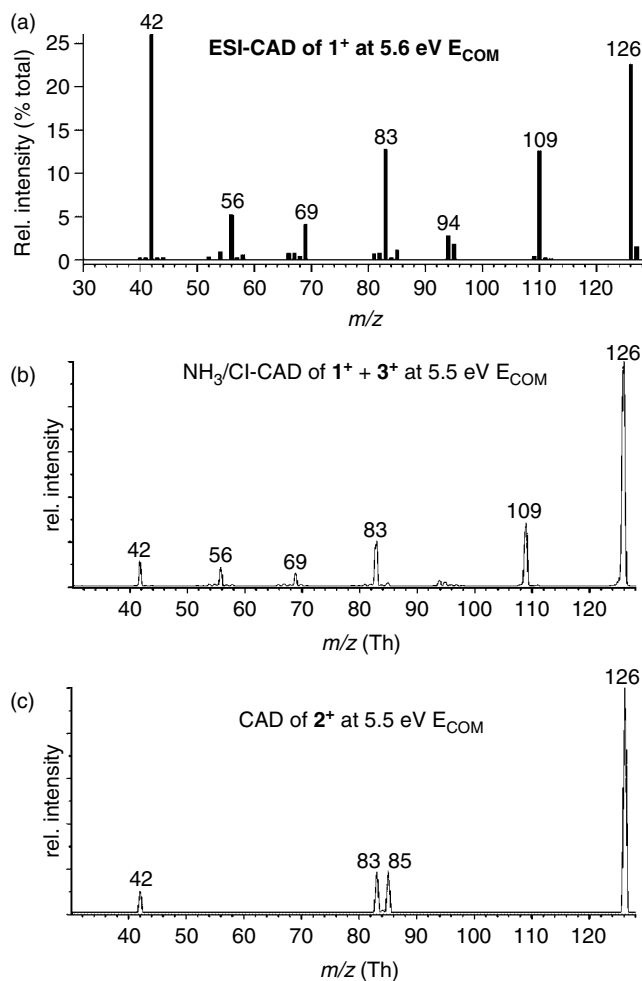
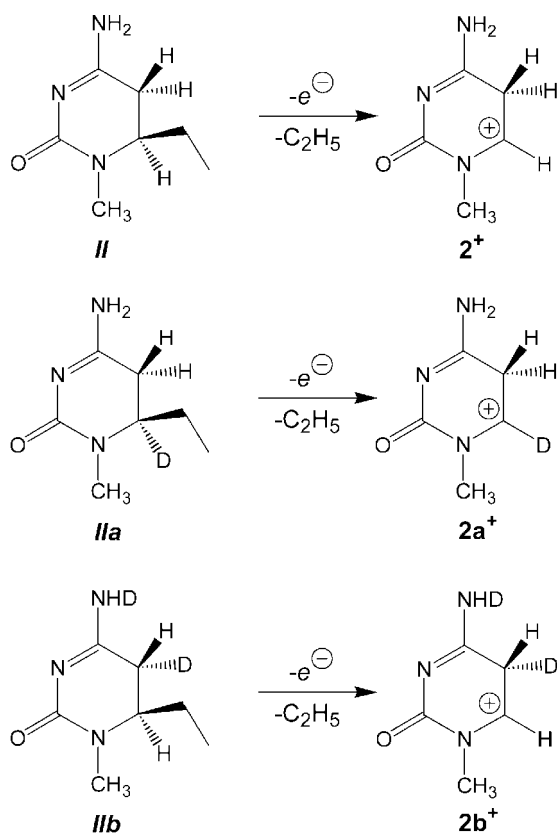


**Figure 2.** Collisionally activated dissociation mass spectra at 5.5–5.6 eV center-of-mass kinetic energy of (a)  $1^+$  by electrospray ionization of *I* in  $\text{CH}_3\text{OH}/\text{H}_2\text{O}$ , (b)  $1^+ + 3^+$  by  $\text{NH}_3/\text{NH}_4^+$  chemical ionization of *I*, (c)  $2^+$  by dissociative ionization of *II*.

shown in Fig. 2(a) and 2(b). The main fragment ions appear at  $m/z$  109 (loss of  $\text{NH}_3$ ), 95, 94, 83, 69, 56, and 42. The CAD spectrum measured on the triple-quadrupole mass spectrometer (Fig. 2(a)) shows higher relative intensities of low-mass fragments (e.g.  $m/z$  42), which is due to the higher pressure of the collision gas used and hence a higher incidence of multiple collisions. Electrospraying *I* from  $\text{CD}_3\text{OD}$  produced very clean ions at  $m/z$  129 ( $1\text{a}^+$ ) that contained three exchangeable deuterons. The CAD spectrum at  $E_{\text{COM}} = 5.4 \text{ eV}$  of  $1\text{a}^+$  showed product ions at  $m/z$  109 (loss of  $\text{ND}_3$ ), 96, 85, 72, 58, 57, and 42 (Fig. 3(a)). These indicated that the elimination of ammonia involved practically exclusively the exchangeable deuterons at N-3 and in the  $\text{ND}_2$  group. The 43-Da neutral fragment that was eliminated to form the  $m/z$  83 ion from  $1^+$  contained only one exchangeable proton (by shift to  $m/z$  85 from  $1\text{a}^+$  that retained two deuterium atoms) and was identified as  $[\text{C}_2\text{H}_2\text{N}_2\text{O}]$  (measured mass 43.0061 Da,  $\text{CHNO}$  requires 43.0058 Da) that most likely involved the N-3 and C-2 ring atoms. By contrast, the  $m/z$  42 fragment ion showed practically no mass shift when produced from  $1\text{a}^+$  and most likely corresponded to  $\text{CH}_3\text{N}=\text{CH}^+$  containing the N-1

methyl and C-6. The CAD spectrum of  $m/z$  129 ions produced by gas-phase deuteration of *I* with  $\text{ND}_4^+$  showed the same fragments as the CAD spectrum of  $1\text{a}^+$  (Fig. 3(b)). Differences are seen in the relative intensities of low-mass fragments that are higher in Fig. 3(a) because of higher incidence of multiple collisions in the triple-quadrupole instrument.

The  $m/z$  126 ions formed by electrospray ionization of *I* are expected to be  $1^+$ , according to the unambiguous energetics of protonation in solution, as discussed above. In contrast, ions produced by mildly exothermic proton transfer to *I* in the gas phase are expected to consist of a mixture of nearly isoenergetic ions  $1^+$  and  $3^+$ . The fact that  $1^+$  and  $(1^+ + 3^+)$  give very similar CAD mass spectra indicates that  $1^+$  and  $3^+$  may interconvert by proton migrations prior to or during dissociation. This can be facilitated by the fact that the main ion dissociations are rearrangements involving proton transfer such as the loss of  $\text{NH}_3$  or ring cleavages.

CAD of  $(1^+ + 3^+)$  at 8 keV kinetic energy results in losses of H ( $m/z$  125),  $\text{CH}_3$  ( $m/z$  111), and formation of several series of fragments in the  $m/z$  94–98, 80–83, 66–70, 52–58, 40–44, and 27–30 ion groups (Fig. 4(a)). Unfortunately, we could not study the 8-keV CAD spectrum of  $1^+$  formed by electrospray to compare it with the CAD spectrum of  $(1^+ + 3^+)$ .

The CAD mass spectrum at  $E_{\text{COM}} = 5.5$  eV of ion  $2^+$  (Fig. 2(c)) is markedly different from the spectra of  $1^+$  or  $(1^+ + 3^+)$ . In particular, ion  $2^+$  dissociates by loss of a 41-Da neutral ( $m/z$  measured as 85.0394,  $\text{C}_3\text{H}_5\text{N}_2\text{O}$  requires 85.0402) that corresponds to  $\text{C}_2\text{H}_3\text{N}$  according to the accurate mass measurements. Note that the  $m/z$  85 fragment is very weak in the CAD spectrum of  $1^+$ . Loss of  $[\text{C}_2\text{H}_3\text{N}, \text{O}]$  ( $m/z$  83) and the formation of the  $m/z$  42 ion ( $\text{C}_2\text{H}_4\text{N}^+$ ) from  $2^+$  are similar to the dissociations of  $1^+$ . However, fragments at

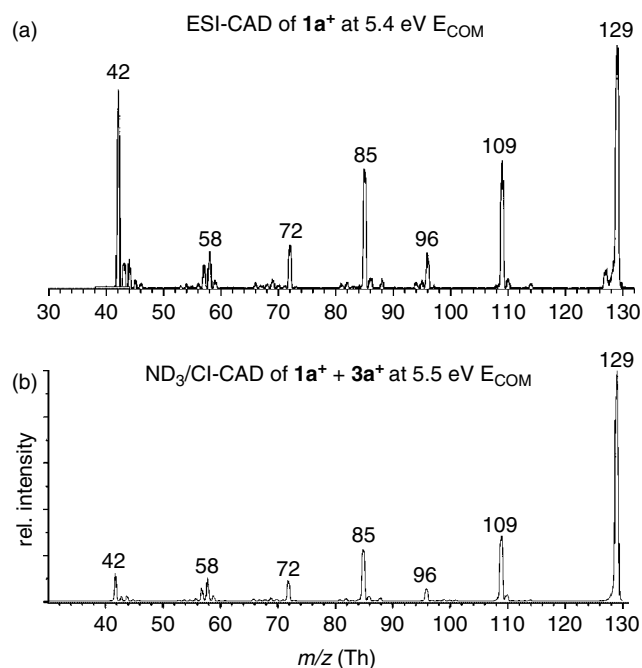


**Figure 3.** Collisionally activated dissociation mass spectra of (a)  $1\text{a}^+$  by electrospray ionization of *I* in  $\text{CD}_3\text{OD}/\text{D}_2\text{O}$  and (b) of  $(1\text{a}^+ + 3\text{a}^+)$  by  $\text{ND}_3/\text{ND}_4^+$  chemical ionization of *I*.

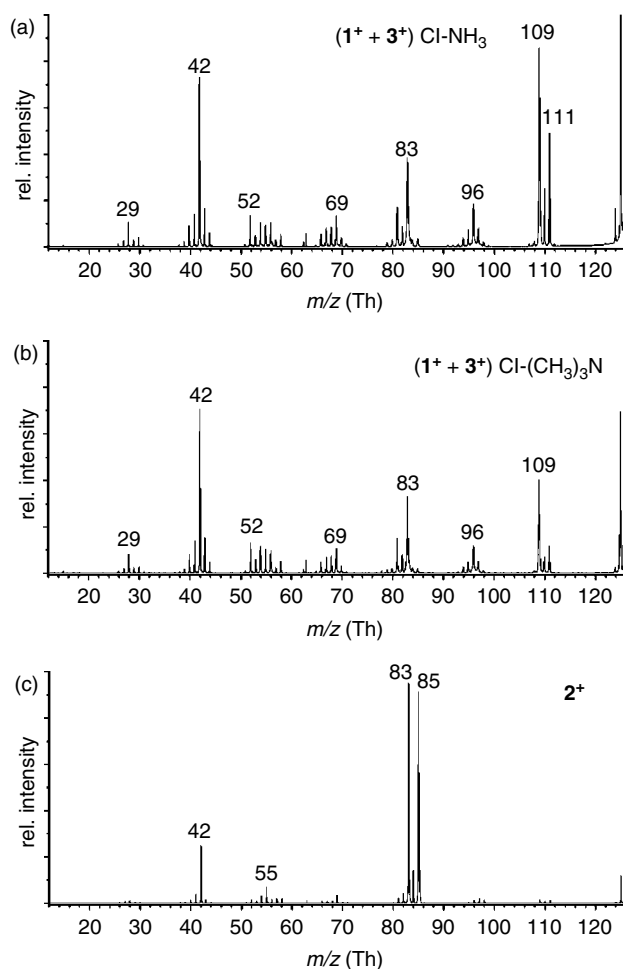


**Figure 4.** Collisionally activated dissociation mass spectra of 8 keV ions. (a)  $(1^+ + 3^+)$  by  $\text{NH}_3/\text{NH}_4^+$  chemical ionization of *I*, (b)  $(1^+ + 3^+)$  by  $(\text{CH}_3)_3\text{N}/(\text{CH}_3)_3\text{NH}^+$  chemical ionization of *I*, and (c)  $2^+$  by dissociative ionization of *II*.

$m/z$  109, 95, 69, and 56, which are characteristic of  $1^+/3^+$ , are practically absent (<1%) in the CAD spectrum of  $2^+$ , indicating that the latter is not contaminated by the much more stable isomers  $1^+$  and  $3^+$ .

Differences were also observed for the 8 keV CAD spectra of  $(1^+ + 3^+)$  and  $2^+$ , as shown in Fig. 4(a–c). Metastable ions  $2^+$  undergo facile elimination of  $\text{C}_2\text{H}_3\text{N}$  and  $\text{HN}=\text{C}=\text{O}$  neutral molecules, so that the  $m/z$  85 and 83 fragment ions dominate the MI-ion spectra. This indicates that eliminations of  $\text{C}_2\text{H}_3\text{N}$  and  $[\text{C}_2\text{H}_3\text{N}, \text{O}]$  are the lowest-energy unimolecular dissociations of  $2^+$ .

Deuterium labeling in  $2\text{a}^+$  and  $2\text{b}^+$  reveals some interesting nuances of ion dissociations.

The CAD spectrum of  $2\text{a}^+$  (Fig. 5(a)) shows loss of a  $\text{C}_2\text{H}_3\text{N}$  molecule that does not contain the 6-D atom. The elimination of  $[\text{C}_2\text{H}_3\text{N}, \text{O}]$  forms the 6-D-containing ion at  $m/z$  84. The  $\text{CH}_3\text{N}=\text{CD}^+$  ion from  $2\text{a}^+$  appears at  $m/z$  43 accompanied by a small satellite at  $m/z$  42 at a  $[m/z\ 43]/[m/z\ 42]$  ratio of 6.3. Taking into account the 2:1 H/D occurrence in the exchange-prone positions C-5 and C-6 in  $2\text{a}^+$ , the fragment ion relative intensities indicate that the ring cleavage resulting in the formation of  $\text{CH}_3\text{N}=\text{CD}^+$  is accompanied by <7% H/D exchange between these

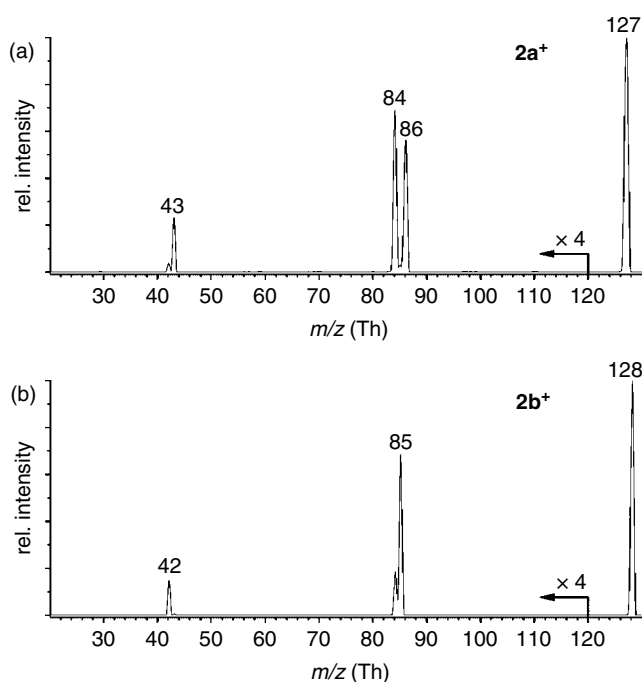


**Figure 5.** Collisionally activated dissociation mass spectra of (a)  $2a^+$  and (b)  $2b^+$  at 5.4–5.5 eV center-of-mass kinetic energy.

positions. The CAD spectrum of  $2b^+$  (Fig. 5(b)) shows loss of a  $C_2HD_2N$  molecule that contains the 5-D and ND atoms. The loss of both  $[C,H,N,O]$  ( $m/z$  85) and  $[C,D,N,O]$  ( $m/z$  84) indicates competing proton and deuteron transfers from the NHD group onto the N-3-C=O fragment during dissociation. The  $CH_3N=CH^+$  ion appears at  $m/z$  42 with  $[m/z\ 42]/[m/z\ 43] = 7.5$ , indicating again that there is little H/D exchange between H-6 and D-5 prior to or during the dissociation.

### Potential energy surfaces for dissociations of $1^+$ and $2^+$

To interpret the CAD spectra and the results of the labeling experiments, we carried out calculations of dissociation and transition state energies for reaction pathways including several ion intermediates. The relative and TS energies are summarized in Tables 3 and 4. The optimized structures of ions  $1^+$ – $5^+$  are depicted in Fig. 6. The reaction scheme for the dissociations of  $1^+$  is shown in Scheme 5. Elimination of ammonia from  $1^+$  is calculated to require an energy of  $374\text{ kJ mol}^{-1}$  at the thermochemical threshold corresponding to the cyclic 1-methyl-4-cytosyl cation ( $8^+$ ). This dissociation threshold is higher than the TS for the reversible isomerization of  $1^+$  and  $3^+$  by 1,3-proton migration,  $E_{TS}(1^+ \rightarrow 3^+) = 153\text{ kJ mol}^{-1}$ . Proton migration from N-3 to the  $NH_2$  group proceeds through a transition state that has  $E_{TS}(1^+ \rightarrow 4^+) = 211\text{ kJ mol}^{-1}$ . Reversible prototropic isomerizations of  $1^+$ ,  $3^+$ , and  $4^+$  are thus possible not only in dissociating ions but also in stable ions of internal energies greater than 153 or  $211\text{ kJ mol}^{-1}$  relative to  $1^+$ . Fragment ion  $8^+$  can isomerize exothermally to an open-chain isomer  $9^+$ , which is  $15\text{ kJ mol}^{-1}$  more stable. While unimolecular  $8^+ \rightarrow 9^+$  isomerization requires additional  $15\text{ kJ mol}^{-1}$  in

**Table 3.** Relative and transition state energies in dissociations of  $1^+$

Species/Reaction	Relative energy <sup>a,b</sup>	
	B3LYP 6-31+G(d,p)	B3-MP2 6-311++G(3df,2p)
$1^+$	0	0
$2^+$	113	111
$3^+$	1.3	-0.2
$4^+$	134	128
$5^+$	161	160
$6^+$	332	350
$7^+$	128	121
$8^+ + NH_3$	387	374
$9^+ + NH_3$	388	358
$10^+$	82	82
$11^+$	258	252
TS( $8^+ \rightarrow 9^+$ )	414	389
TS( $1^+ \rightarrow 3^+$ )	152	153
TS( $1^+ \rightarrow 4^+$ )	214	211
TS( $1^+ \rightarrow 10^+$ )	333	323
TS( $10^+ \rightarrow 11^+$ )	350	352
$12^+ + HO-C\equiv N$	324	321
$13^+ + HN=C=O$	334	342
$12^+ + HN=C=O$	207	206
$CH_2=C=NH_2^+ +$	429	437
$CH_3N\equiv C + HN=C=O$		
$CH_3N\equiv CH^+ +$	359	342
$CH_2=C(NH_2)N=C=O$		
$CH_3N\equiv CH^+ + 20$	428	419

<sup>a</sup> In units of  $\text{kJ mol}^{-1}$ .

<sup>b</sup> Including B3LYP/6-31+G(d,p) zero-point vibrational energies and referring to 0 K.

the transition state, the isomerization can be possibly facilitated by the ammonia molecule. Details of such a catalyzed isomerization<sup>45</sup> have not been studied in this work.

The competing formation of  $CH_3N\equiv CH^+$  at  $m/z$  42 probably involves hidden proton transfers in the neutral fragment to form a stable molecule. For example, H-migration from N-3 to C-5 can form  $CH_2=C(NH_2)N=C=O$  (**20**) and  $CH_3N\equiv CH^+$  at  $342\text{ kJ mol}^{-1}$  threshold energy, which is competitive with the elimination of ammonia from  $1^+$  (Table 3). Other dissociation mechanisms leading to cyclic neutral fragments (**21**) or formation of  $CH_2=C=NH_2^+$  (Scheme 5) require higher threshold energies and are likely to be disfavored.

The elimination of  $[C,H,N,O]$  shows some interesting features (Fig. 7). Ring opening by an N-1-C-2 bond cleavage in  $1^+$  requires a fairly high energy in TS ( $(1^+ \rightarrow 10^+)$ ,  $E_{TS} = 323\text{ kJ mol}^{-1}$ ) forming intermediate  $10^+$  at  $82\text{ kJ mol}^{-1}$  relative to  $1^+$ . Upon breaking the N-3-C-4 bond, the N-C-O fragment develops hydrogen bonds to both N-1-H and N-7-H protons in the transition state TS ( $10^+ \rightarrow 11^+$ ). Interestingly, the minimum energy reaction path from this TS leads to a transfer of N-7-H, not N-1-H, forming the ion-molecule complex  $11^+$ . This pathway was confirmed by intrinsic reaction coordinate calculations<sup>46</sup> starting in

**Table 4.** Relative and transition state energies in dissociations of  $2^+$

Species/Reaction	Relative energy <sup>a,b</sup>	
	B3LYP 6-31+G(d,p)	B3-MP2 6-311++G(3df,2p)
$2^+$	0	0
TS( $2^+ \rightarrow 4^+$ )	234	236
$14^+$	23	20
TS( $2^+ \rightarrow 14^+$ )	56	51
$15^+$	23	19
TS( $15^+ \rightarrow 16^+$ )	24	21
$16^+$	68	65
TS( $16^+ \rightarrow 17^+$ )	202	191
$17^+$	176	152
TS( $17^+ \rightarrow$	196	189
$18^+ + \text{CH}_2=\text{C}=\text{NH}$ )		
$18^+ + \text{CH}_2=\text{C}=\text{NH}$	177	179
$19^+ + \text{O}=\text{C}=\text{NH}$	189	175
$12^+ + \text{O}=\text{C}=\text{NH}$	71	75

<sup>a</sup> In units of  $\text{kJ mol}^{-1}$ .

<sup>b</sup> Including B3LYP/6-31+G(d,p) zero-point vibrational energies and referring to 0 K.

TS( $10^+ \rightarrow 11^+$ ). Further dissociation of  $11^+$  leads to the formation of ion  $12^+$  and  $\text{HO}-\text{C}\equiv\text{N}$  at  $321 \text{ kJ mol}^{-1}$  threshold energy. Note that the alternative elimination

of  $\text{HN}=\text{C}=\text{O}$  with transfer of the N-1-H proton would require  $342 \text{ kJ mol}^{-1}$  threshold energy forming ion  $13^+$ ,  $[\text{H}_2\text{N}=\text{C}=\text{CH}-\text{CH}=\text{N}-\text{CH}_3]^+$ , which is  $21 \text{ kJ mol}^{-1}$  above the threshold energy for  $12^+ + \text{HO}-\text{C}\equiv\text{N}$  (Table 3). The formation of the most stable neutral ( $\text{HN}=\text{C}=\text{O}$ ) and ion fragments ( $12^+$ ) would have the lowest threshold at  $206 \text{ kJ mol}^{-1}$ , but is mechanistically impossible from  $11^+$ , unless  $\text{HO}-\text{C}\equiv\text{N}$  undergoes isomerization in an ion-molecule complex. Overall, the mechanistic subtleties in the exit channel are rather moot, because the dissociation kinetics are likely to be controlled by the flux through the rate-determining step in the highest-energy TS ( $10^+ \rightarrow 11^+$ ).

Dissociation of ion  $2^+$  starts by breaking the weak N-1-C-2 bond, which is substantially elongated in  $2^+$  ( $1.571 \text{ \AA}$ ) (Fig. 6). This bond dissociation requires only  $51 \text{ kJ mol}^{-1}$  in the TS and forms the isomeric cation  $14^+$  (Scheme 6), which is only  $20 \text{ kJ mol}^{-1}$  less stable than  $2^+$  (Table 4). Intermediate  $14^+$  can further rearrange by a practically barrierless proton transfer to ion  $15^+$ . Internal bond rotation in the latter forms a less stable intermediate ( $16^+$ ) that can undergo isomerization by a migration of the  $\text{O}=\text{C}=\text{N}$  group ( $17^+$ ), followed by loss of a  $\text{CH}_2=\text{C}=\text{NH}$  molecule forming the  $m/z$  85 ion ( $18^+$ ) at  $179 \text{ kJ mol}^{-1}$  threshold energy. The kinetic bottlenecks of the overall sequence are at TS( $16^+ \rightarrow 17^+$ ) and TS( $17^+ \rightarrow 18^+ + \text{CH}_2=\text{C}=\text{NH}$ ), which are, respectively,  $191$  and  $189 \text{ kJ mol}^{-1}$  above  $2^+$ . An interesting feature of the chemistry of  $2^+$  is that it and structures  $14^+$  and  $15^+$  can coexist at equilibrium at relatively low internal energies above  $E_{\text{TS}}(2^+ \rightarrow 14^+) = 51 \text{ kJ mol}^{-1}$ . Intermediates

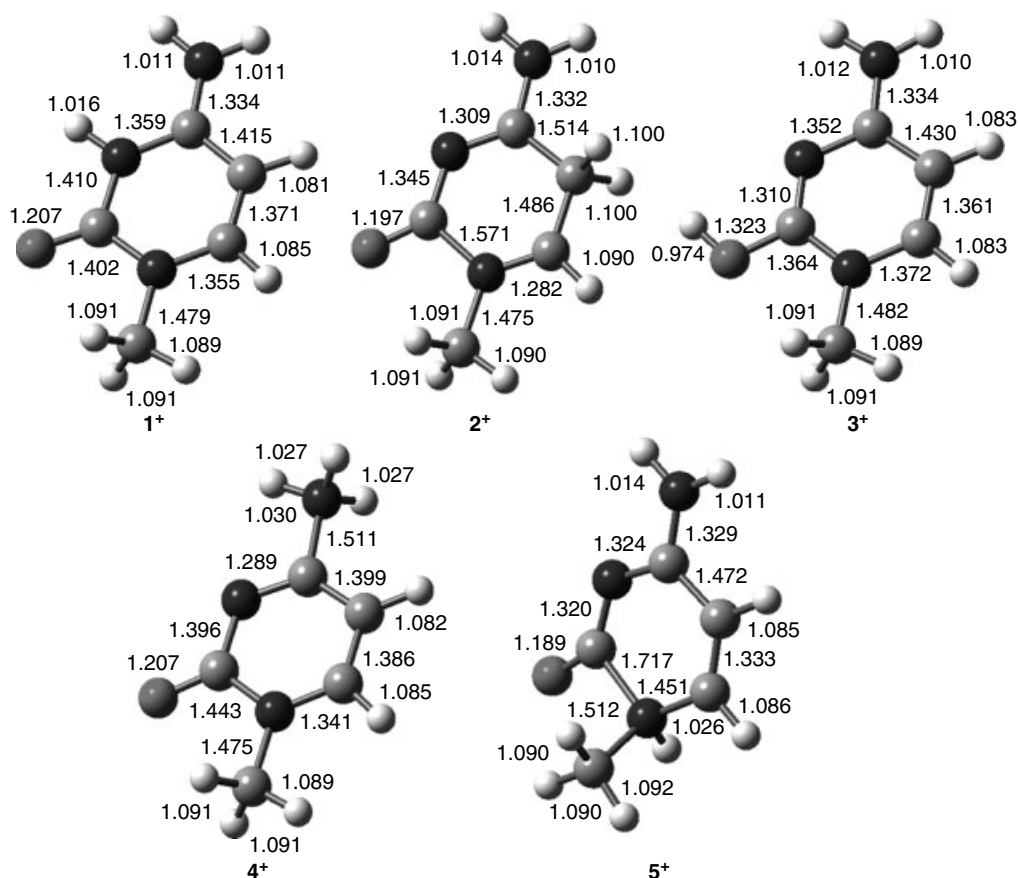
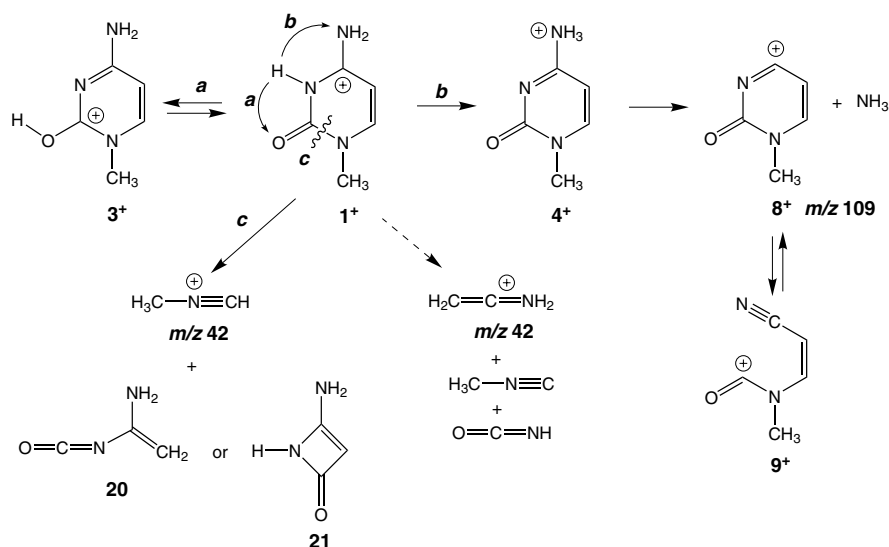


**Figure 6.** B3LYP/6-31+G(d,p) optimized structures of ions  $1^+ - 5^+$ . Bond lengths in angstroms.



Scheme 5

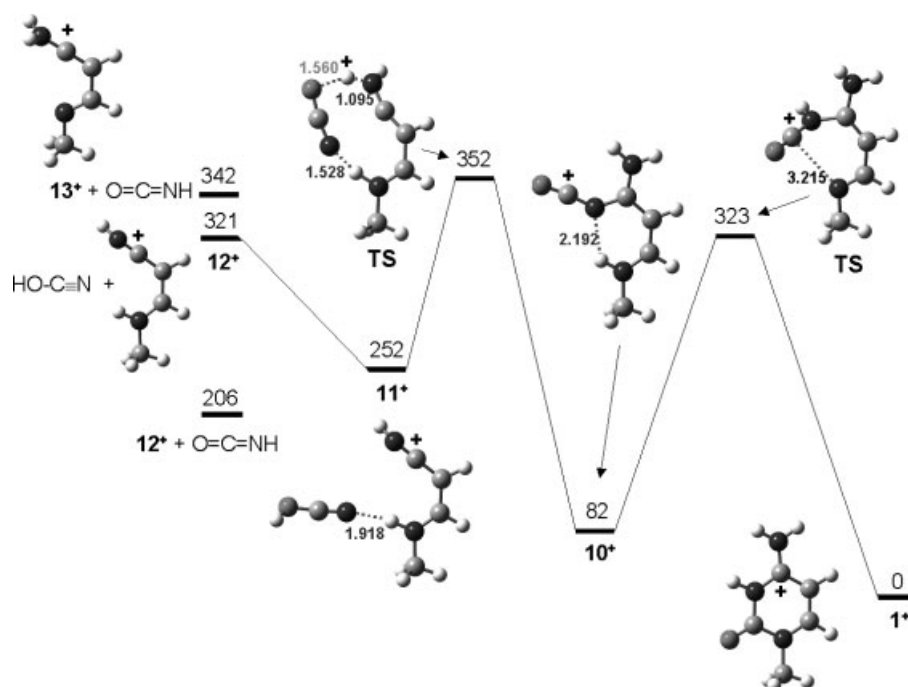


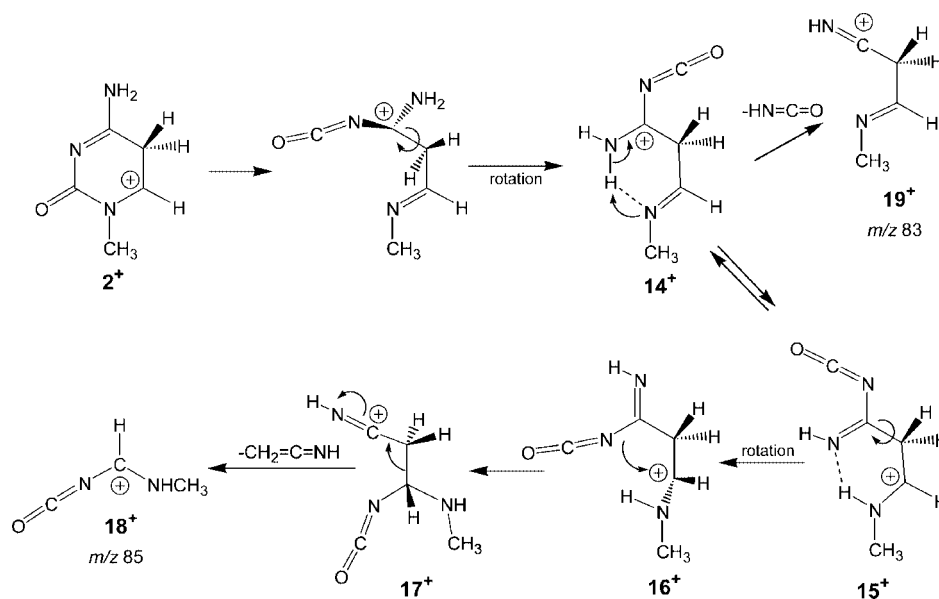
**Figure 7.** Optimized structures and potential energy profile for dissociations of  $1^+$ . The energies are from B3-MP2/6-311++G(3df,2p) single-point calculations and include B3LYP/6-31+G(d,p) zero-point vibrational corrections.

$14^+$  and  $15^+$  are conceivable as branching points for the competing elimination of  $\text{HN}=\text{C}=\text{O}$  from  $2^+$ . For example, the thermochemical threshold for the formation of ion  $19^+$  by  $\text{HN}=\text{C}=\text{O}$  elimination from  $14^+$  is at 175 kJ mol<sup>-1</sup> relative to  $2^+$  (Scheme 6). The threshold for  $\text{HN}=\text{C}=\text{O}$  elimination from  $15^+$  to form ion  $12^+$  is only 75 kJ mol<sup>-1</sup> relative to  $2^+$  (Table 4). Note, however, that both eliminations require 1,3-proton migrations to form the  $\text{HN}=\text{C}=\text{O}$  molecule and are likely to require additional energy in the respective transition states.

## CONCLUSIONS

A proper design of ionization methods and ion chemistry allowed us to selectively generate two tautomers of

protonated 1-methylcytosine and show that they were distinct species. The N-3-protonated tautomer  $1^+$  can undergo prototropic isomerization to the isoenergetic O-2-protonated tautomer  $3^+$  prior to dissociation by loss of ammonia. The competitive elimination of a [C,H,N,O] neutral molecule is predicted to form  $\text{HO}-\text{C}\equiv\text{N}$ , not the more stable  $\text{HN}=\text{C}=\text{O}$ . The dissociation mechanism is driven by the thermochemistry of the fragment ions, not neutral molecules. The C-5-protonated tautomer  $2^+$  undergoes facile ring opening and dissociates by competitive eliminations of  $\text{HN}=\text{C}=\text{O}$  and  $\text{CH}_2=\text{C}=\text{NH}$  molecules. This study shows that seemingly simple dissociations of nucleobase cations involve multistep mechanisms and result in the formation of unexpected fragments.



Scheme 6

## Acknowledgements

F. T. thanks the National Science Foundation for generous funding through grants CHE-0349595 for experiments and CHE-0342956 for computations. Support for the Computational Chemistry Facility at the Department of Chemistry was jointly provided by the NSF and University of Washington. M. P. thanks the Grant Agency of the Czech Republic (Grant No. 203/02/0737) and the Grant Agency of the Academy of Sciences of the Czech Republic (Grant No. IAA400400502) for financial support.

## REFERENCES

- McCloskey JA. Constituents of nucleic acids. Overview and strategy. *Methods Enzymol*, vol. 193, McCloskey JA (ed). Academic Press: San Diego, 1990; Section IV, Nucleic Acid Constituents, 771.
- Nelson CC, McCloskey JA. Collision-induced dissociation of uracil and its derivatives. *J. Am. Soc. Mass Spectrom.* 1994; **5**: 339.
- Nelson CC, McCloskey JA. Collision-induced dissociation of adenine. *J. Am. Chem. Soc.* 1992; **114**: 3661.
- Gregson JM, McCloskey JA. Collision-induced dissociation of protonated guanine. *Int. J. Mass Spectrom. Ion Process.* 1997; **165/166**: 475.
- Tureček F, Chen X. Protonated adenine: tautomers, solvated clusters, and dissociation mechanisms. *J. Am. Soc. Mass Spectrom.* 2005; **16**: 1713.
- Szczesniak M, Szczepaniak K, Kwiatkowski JS, Kubulat K, Person WB. Matrix isolation infrared studies of nucleic acid constituents. 5. Experimental matrix-isolation and theoretical ab initio SCF molecular orbital studies of the infrared spectra of cytosine monomers. *J. Am. Chem. Soc.* 1988; **110**: 8319.
- Person WB, Szczepaniak K, Szczesniak M, Kwiatkowski JS, Hernandez L, Czerminski R. Tautomerism of nucleic acid bases and the effect of molecular interactions on tautomeric equilibria. *J. Mol. Struct.* 1989; **194**: 239.
- Kobayashi R. A CCSD(T) study of the relative stabilities of cytosine tautomers. *J. Phys. Chem. A* 1998; **102**: 10 813.
- Fogarasi G. High-level electron correlation calculations on some tautomers of cytosine. *J. Mol. Struct.* 1997; **413–414**: 271.
- Hall RJ, Burton NA, Hiller IH, Young PE. Tautomeric equilibria in 2-hydroxypyridine and in cytosine. An assessment of density functional methods, including gradient corrections. *Chem. Phys. Lett.* 1994; **220**: 129.
- Trygubenko SA, Bogdan TV, Rueda M, Orozco M, Luque FJ, Šponer J, Slavíček P, Hobza P. Correlated ab initio study of nucleic acid bases and their tautomers in the gas phase, in a microhydrated environment and in aqueous solution. *Phys. Chem. Chem. Phys.* 2002; **4**: 4192.
- Tureček F, Yao C. Hydrogen atom addition to cytosine, 1-Methylcytosine, and cytosine-water complexes. A computational study of a mechanistic dichotomy. *J. Phys. Chem. A* 2003; **107**: 9221.
- Chen X, Syrstad EA, Gerbaux P, Nguyen MT, Tureček F. Distonic isomers and tautomers of adenine cation radical in the gas phase and aqueous solution. *J. Phys. Chem. A* 2004; **108**: 9283.
- Szczesniak M, Leszczynski J, Person WB. Identification of the imino-oxo form of 1-methylcytosine. *J. Am. Chem. Soc.* 1992; **114**: 2731.
- Tureček F. Modeling Nucleobase Radicals in the Mass Spectrometer. *J. Mass Spectrom.* 1998; **33**: 779.
- Tureček F. Generation and characterization of transient intermediates by neutralization-reionization mass spectrometry. In *Encyclopedia of Mass Spectrometry*, vol. 1 Armentrout PB (ed). Elsevier: Amsterdam, 2003; Chapt. 8; 528.
- Tureček F. Transient intermediates of chemical reactions by neutralization-reionization mass spectrometry. *Top. Curr. Chem.* 2003; **225**: 77.
- Hosmane RS, Leonard NJ. Simple convenient synthesis of 1-methylcytosine. *Synthesis* 1981; 118.
- McFadden HG, Huppertz JL. Synthesis of (Pyrazol-4-yl)alkanones and Alkylpyrazole-4-carbonitriles. *Aust. J. Chem.* 1991; **44**: 1263.
- Krapcho AP. Synthetic applications of dealkoxycarbonylations of Malonate Esters,  $\beta$ -Keto Esters,  $\alpha$ -Cyano Esters and related compounds in dipolar aprotic media – Part II. *Synthesis* 1982; 893.
- Borch RF. Reductive amination with sodium cyanoborohydride: N,N-dimethylcyclohexylamine. *Org. Synth.* 1982; **52**: 124.
- Borch RF, Hassid AI. A new method for the methylation of amines. *J. Org. Chem.* 1981; **37**: 1673.
- Ingersoll AW, Armendt BF. Nitrourea. *Org. Synth. Coll.* 1941; **I**: 417.
- Brown DM, Hewlins MJE. Dihydrocytosine and related compounds. *J. Chem. Soc. C* 1968; 2050.
- Frisch MJ, Trucks GW, Schlegel HB, Scuseria GE, Robb MA, Cheeseman JR, Montgomery JA Jr, Vreven T, Kudin KN, Burant JC, Millam JM, Iyengar SS, Tomasi J, Barone V, Mennucci B, Cossi M, Scalmani G, Rega N, Petersson GA, Nakatsuji H, Hada M, Ehara M, Toyota K, Fukuda R, Hasegawa J, Ishida M, Nakajima T, Honda Y, Kitao O, Nakai H, Klene M, Li X, Knox JE, Hratchian HP, Cross JB, Adamo C, Jaramillo J, Gomperts R, Stratmann RE, Yazyev O, Austin AJ, Cammi R,

- Pomelli C, Ochterski JW, Ayala PY, Morokuma K, Voth GA, Salvador P, Dannenberg JJ, Zakrzewski VG, Dapprich S, Daniels AD, Strain MC, Farkas O, Malick DK, Rabuck AD, Raghavachari K, Foresman JB, Ortiz JV, Cui Q, Baboul AG, Clifford S, Cioslowski J, Stefanov BB, Liu G, Liashenko A, Piskorz P, Komaromi I, Martin RL, Fox DJ, Keith T, Al-Laham MA, Peng CY, Nanayakkara A, Challacombe M, Gill PMW, Johnson B, Chen W, Wong MW, Gonzalez C, Pople JA. *Gaussian 03, Revision B.05*. Gaussian: Pittsburgh, PA, 2003.
26. Becke AD. A new mixing of hartree-fock and local-density-functional theories. *J. Chem. Phys.* 1993; **98**: 1372.
  27. Becke AD. Density functional thermochemistry III. The role of exact exchange. *J. Chem. Phys.* 1993; **98**: 5648.
  28. Stephens PJ, Devlin FJ, Chabalowski CF, Frisch MJ. Ab initio calculation of vibrational absorption and circular dichroism spectra using density functional force fields. *J. Phys. Chem.* 1994; **98**: 11 623.
  29. Møller C, Plesset MS. Note on an approximation treatment for many-electron systems. *Phys. Rev.* 1934; **46**: 618.
  30. Tureček F. Proton affinity of dimethyl sulfoxide and relative stabilities of  $C_2H_6OS$  molecules and  $C_2H_7OS^+$  ions. A comparative G2(MP2) ab initio and density functional theory study. *J. Phys. Chem. A* 1998; **102**: 4703.
  31. Tureček F, Wolken JK. Dissociation energies and kinetics of aminopyrimidinium radicals by ab initio and density functional theory. *J. Phys. Chem. A* 1999; **103**: 1905.
  32. Rablen PR. Is the acetate anion stabilized by resonance or electrostatics? A systematic structural comparison. *J. Am. Chem. Soc.* 2000; **122**: 357.
  33. Tureček F, Wolken JK, Sadílek M. Distinction of isomeric pyridyl cations and radicals by neutralization-reionization mass spectrometry, ab initio and density functional theory calculations. *Eur. Mass Spectrom.* 1998; **4**: 321.
  34. Wolken JK, Tureček F. Heterocyclic radicals in the gas phase. An experimental and computational study of 3-hydroxypyridinium radicals and cations. *J. Am. Chem. Soc.* 1999; **121**: 6010.
  35. Wolken JK, Tureček F. Modeling nucleobase radicals in the gas phase. Experimental and computational study of 2-hydroxypyridinium and 2(1H)-pyridone radicals. *J. Phys. Chem. A* 1999; **103**: 6268.
  36. Tureček F, Carpenter FH. Glycine radicals in the gas phase. *J. Chem. Soc., Perkin Trans. 2* 1999; 2315.
  37. Polášek M, Tureček F. Hydrogen atom adducts to nitrobenzene: formation of the phenylnitronic radical in the gas phase and energetics of wheland intermediates. *J. Am. Chem. Soc.* 2000; **122**: 9511.
  38. Rablen PR, Benstrup KH. Are the enolates of amides and esters stabilized by electrostatics? *J. Am. Chem. Soc.* 2003; **125**: 2142.
  39. Tomasi J, Cammi R, Mennucci B, Cappelli C, Corni S. Molecular properties in solution described with a continuum solvation model. *Phys. Chem. Chem. Phys.* 2002; **4**: 5697.
  40. Cossi M, Scalmani G, Rega N, Barone V. New developments in the polarizable continuum model for quantum mechanical and classical calculations on molecules in solution. *J. Chem. Phys.* 2002; **117**: 43.
  41. Barone V, Cossi M, Tomasi J. A new definition of cavities for the computation of solvation free energies by the polarizable continuum model. *J. Chem. Phys.* 1997; **107**: 3210.
  42. Becker ED, Miles HT, Bradley RB. Nuclear magnetic resonance studies of methyl derivatives of cytosine. *J. Am. Chem. Soc.* 1965; **87**: 5575.
  43. Gatlin CL, Tureček F. Acidity determination in droplets formed by electro spraying methanol-water solutions. *Anal. Chem.* 1994; **66**: 712.
  44. McLafferty FW, Tureček F. *Interpretation of Mass Spectra*, 4th ed. University Science Books: Sausalito, 1993.
  45. Tureček F, Drinkwater DE, McLafferty FW. The stepwise nature of the  $\gamma$ -hydrogen rearrangement in unsaturated ions. *J. Am. Chem. Soc.* 1990; **112**: 993.
  46. Gonzalez C, Schlegel HB. Reaction path following in mass-weighted internal coordinates. *J. Phys. Chem.* 1990; **94**: 5523.